

1 Removal mechanism and quantitative control of trichloroethylene in
2 post-plasma-catalytic system over Mn-Ce/HZSM-5 catalysts

3 Tian Chang^{1,2,3,4}, Qingcai Chen¹, Hao Fan², Zhenxing Shen^{2*}, Bin Zhang², Yu Huang⁴,
4 Savita K.P. Veerapandian³, Nathalie De Geyter³, Rino Morent³

5
6
7
8
9 ¹ *School of Environmental Science and Engineering, Shaanxi University of Science
10 and Technology, Xi'an 710021, China*

11 ² *Department of Environmental Science and Engineering, Xi'an Jiaotong University,
12 Xi'an 710049, China*

13 ³ *Research Unit Plasma Technology, Department of Applied Physics, Faculty of
14 Engineering and Architecture, Ghent University, Sint-Pietersnieuwstraat 41 – B4,
15 9000 Ghent, Belgium*

16 ⁴ *Key Lab of Aerosol Chemistry & Physics, SKLLQG, Institute of Earth Environment,
17 Chinese Academy of Sciences, Xi'an 710049, China*

18

19

20 **Author to whom correspondence should be addressed. E-mail:*

21 *zxshen@mail.xjtu.edu.cn (Zhenxing Shen), +86 18792765891.*

22

23 **Text S1 The calculation method of TCE removal efficiency, CO₂ yield and CO**
24 **yield**

25 The TCE removal efficiency (η_{TCE}), CO₂ yield (Y_{CO_2}) and CO yield (Y_{CO}) were
26 calculated as follows:

27
$$\eta_{\text{TCE}}(\%) = \frac{[\text{TCE}]_{\text{inlet}} - [\text{TCE}]_{\text{outlet}}}{[\text{TCE}]_{\text{inlet}}} \times 100\% \quad (1)$$

28
$$Y_{\text{CO}_2}(\%) = \frac{[\text{CO}_2]}{2[\text{TCE}]_{\text{inlet}}} \times 100\% \quad (2)$$

29
$$Y_{\text{CO}}(\%) = \frac{[\text{CO}]}{2[\text{TCE}]_{\text{inlet}}} \times 100\% \quad (3)$$

30 where $[\text{TCE}]_{\text{inlet}}$ and $[\text{TCE}]_{\text{outlet}}$ are denoted as the TCE concentrations at the inlet and
31 outlet of the reactor, respectively; $[\text{CO}_2]$ and $[\text{CO}]$ are represented as the CO₂ and CO
32 concentrations at the exit of the reactor, respectively.

33

34 **Text S2 Electrical measurement method**

35 The reactor was connected to a DC high voltage power supply (SR40-R-1200,
36 Technix). A high voltage probe (Fluke 80 K-40, division ratio 1/1000) was used to
37 measure the applied voltage. The discharge current was determined by monitoring the
38 voltage signal across a 100 Ω resistor which was put in series between the counter
39 electrode and ground. The discharge power (P) was calculated using the applied
40 voltage (U) and the reactor current (I) according to the Eq. (4).

41
$$P(\text{W}) = U \times I \quad (4)$$

42

43 **Text S3 Catalyst preparation and characterization**

44 The Mn-Ce/HZSM-5 (molar ratio of Ce/Mn=0.2, 0.6, 1 and 1.4) catalysts were
45 prepared using the deposition–precipitation method. A typical synthesis of Mn-
46 Ce/HZSM-5 contained the following steps. The $\text{Ce}(\text{NO}_3)_3 \cdot 6\text{H}_2\text{O}$ and $\text{Mn}(\text{NO}_3)_2$ were
47 dissolved in deionized water with continuous stirring. Then, HZSM-5, KMnO_4 and
48 Na_2CO_3 were added to the above mixture successively under stirring. Subsequently,

49 the obtained mixture aged for 4 h at 60 °C. Finally, the above mixture was filtered,
50 dried overnight at 70 °C, followed by calcination in air at 500 °C for 3 h. The catalyst
51 samples were donated as MnCe_x, where x stood for the molar ratio of Ce/Mn.

52 The XRD patterns of all the prepared samples were analyzed by a X-ray powder
53 diffractometer (PAN analytical, X'pert, Almelo) equipped with a Cu-Kα radiation
54 source (λ = 1.5406 Å). The Raman spectra were acquired on Confocal Raman
55 spectroscopy (Lab RAM, HR 800, Horiba, France) using the 514.0 nm radiation from
56 an argon laser. The quantitative analysis of the element content of all the prepared
57 samples used an inductively coupled plasma emission spectrometry (E 9000,
58 Shimadzu). The specific surface area, total pore volume and average pore diameter of
59 all the prepared samples were obtained via N₂ adsorption–desorption isotherms at 77
60 K using an SSA-4200 analyzer (Beijing Builder). The morphology of all the prepared
61 samples was recorded through field-emission scanning electron microscopy (SEM
62 500, Gemini). The high-resolution transmission electron microscopy (HR-TEM) was
63 used to measure the dispersion and configuration of catalysts (JEOL, Model JEM-
64 2100HR instrument, Japan). H₂-TPR and NH₃-TPD of all the prepared samples were
65 both operated on the same Micromeritics AutoChem 2910 instrument equipped with a
66 thermal conductivity detector (TCD), with 0.05 g catalyst for H₂-TPR and 0.1 g
67 catalyst for NH₃-TPD. XPS was conducted at room temperature on AXIS ULtrabl
68 XPS (ESCALAB Xi+, Thermo Fisher Scientific) equipment to analyze the oxidation
69 states of the elements. The C1s photoelectron peak at 284.8 eV was used to check the
70 binding energy (BE) calibration.

71

72 **Text S4 The second-order polynomial used to fit the modelling response variable**

73

$$Y = \beta_0 + \sum_{i=1}^k \beta_i X_i + \sum_{i=1}^k \beta_{ii} X_i^2 + \sum_{i=1}^{k-1} \sum_{j=2}^k \beta_{ij} X_i X_j + \varepsilon \quad (5)$$

74 Y: the predicted response; k: the number of variables, ε: the residual value; β₀: the
75 constant; β_i: the linear coefficient; β_{ii}: the quadratic coefficient; β_{ij}: the interaction
76 coefficient; X_i, X_j: the coded independent variables.

77 Figure Captions

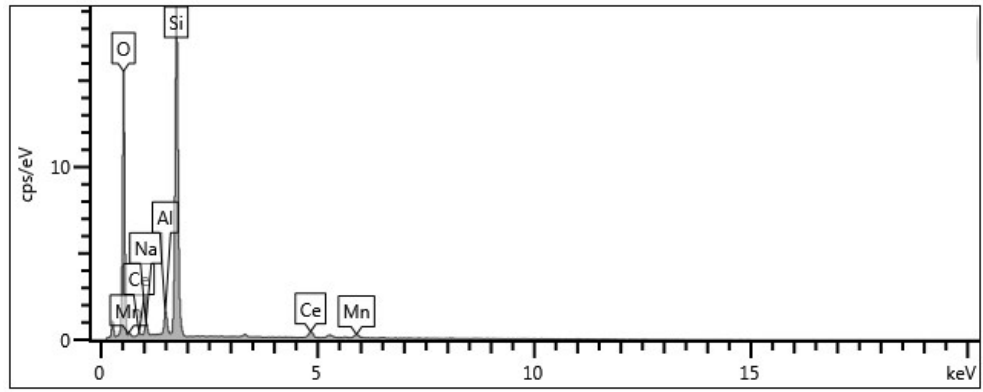
78 Fig. S1. EDX mapping of MnCe₁ sample.

79 Fig. S2. Predicted and actual results of (a) TCE removal efficiency, (b) CO₂ yield and

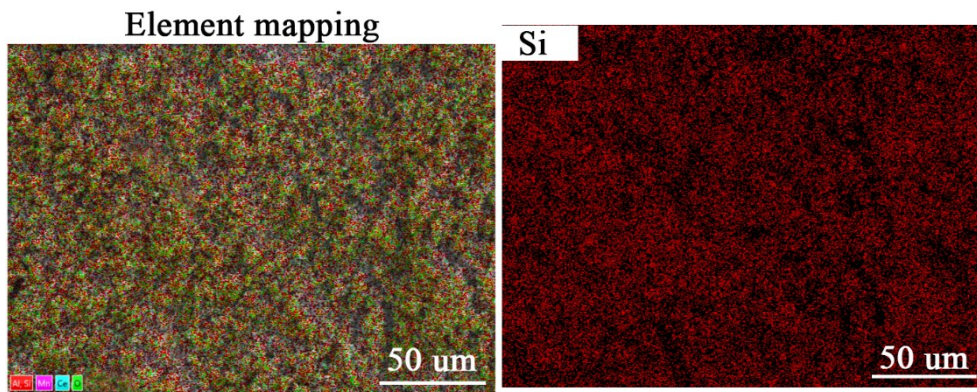
80 (c) CO yield.

81

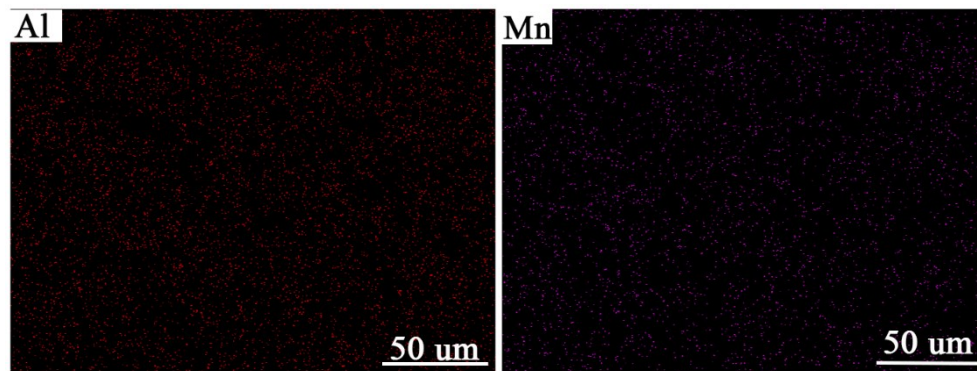
82



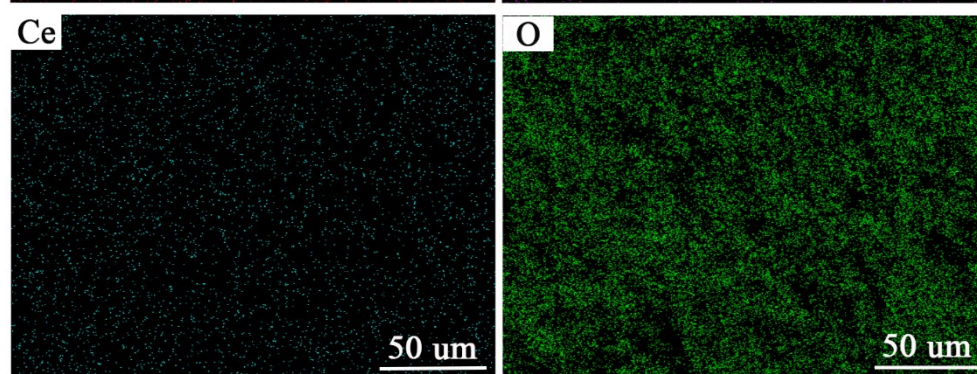
83



84



85



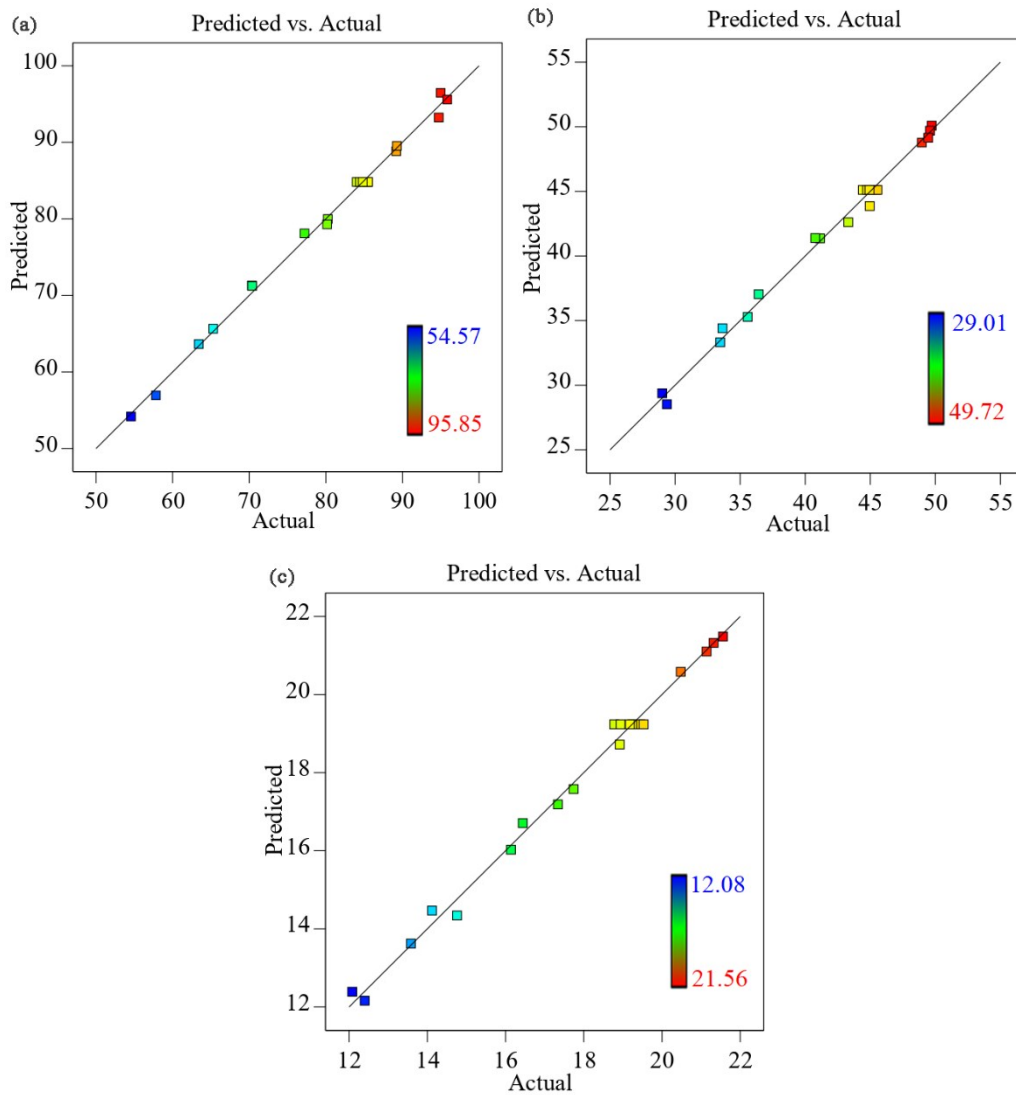
86

Fig. S1. EDX mapping of MnCe₁ sample.

87

88

89



90

91

92 Fig. S2. Predicted and actual results of (a) TCE removal efficiency, (b) CO₂ yield and (c) CO yield.

93